

Stability and non-linear response of 1D microfluidic-particle streams

Nicolas Champagne,^a Eric Lauga,^b and Denis Bartolo^a

Received Xth XX 2011, Accepted Xth XX 20XX

First published on the web Xth XX 20XX

DOI: 10.1039/xx

We study the dynamic response of 1D microfluidic-droplet streams to finite-amplitude longitudinal perturbations. We demonstrate experimentally that the excitation of localized jams results in the propagation of shock waves. The shock velocity is shown to vanish as the average particle density approaches a critical value thereby leaving long-lived disturbance in the spatial organization of the streams. Using a gradient expansion of the hydrodynamic coupling between the advected particles, we then theoretically derive the nonlinear constitutive equation relating particle current to particle density, and show that it leads to Burgers equation for the droplet stream density.

Numerous microfluidic techniques rely on the streaming of particles in microchannels. In flow cytometry devices, focused streams of microparticles such as cells and colloids are sorted and analysed¹. In droplet-based devices², liquid droplets are produced and transported at high rates – up to several kHz – and the resulting one-dimensional (1D) droplet crystals form a useful collection of independent microreactors to perform parallel chemical reactions. In the engineering of functional polymeric particles, either by polymerizing prepolymer-based droplets or *in situ* lithographic techniques³, one-dimensional streams of solid particles are typically created, and handled in shallow microchannels. As these applications are intended to yield high-throughput analysis, controlling the stability of the 1D streams of microfluidic particles can be a major issue. Several solutions exist to enhance the robustness of the particle transport with respect to transverse perturbations, e.g. using guiding rails along the microchannels^{4,6}. However, the stabilization with respect to longitudinal perturbations remains an unsolved problem.

From a fundamental perspective, our understanding of particle transport in microchannels has mostly focused on hydrodynamic phenomena occurring at the single-particle level, including droplet formation and breaking, inertial effects, and lubrication-induced deformations⁵. In contrast, little work has been devoted to the large scale dynamics of 1D particle

streams. Notable exceptions include the investigations of Beatus and coworkers, who demonstrated that 1D droplet crystals are linearly stable, with small perturbations propagating while leaving the crystalline order unchanged^{7,8}. In recent work, we have shown that there exists a maximal bound for the stationary current of 1D particle streams driven in Hele-Shaw geometries and in obstacle networks⁹. When the (imposed) particle current exceeds this critical value, long-range hydrodynamic interactions between the advected particles lead to the spontaneous formation of jams, resulting in the longitudinal and the subsequent transverse destabilization of the 1D streams.

In this paper, we study the dynamic response of regular 1D streams (crystals) to finite-amplitude longitudinal perturbations. Using a microfluidic device, we show that the excitation of localized jams results in the propagation of shock waves whose speed vanishes as the average particle density approaches a critical value, thereby leaving long lived disturbance in the spatial organization of the crystals. To account theoretically for this nonlinear dynamics, we use a gradient expansion of the hydrodynamic coupling between the advected particles to derive the nonlinear constitutive equation relating particle current to particle density. Our results show that the polar symmetry of the hydrodynamic interaction kernel governs the dynamic response and the stability of 1D streams.

Our experiment consists in flowing a 1D crystal made by injecting droplets at a constant rate in a straight channel, as illustrated in Fig. 1. We then suddenly increase the injection rate for a short period of time, thereby creating a localized jam along the particle stream. The dynamic response of the stream to this longitudinal perturbation is characterized by analyzing the spatiotemporal evolution of the droplet packing fraction.

The device is a microfluidic sticker made of thiolene based

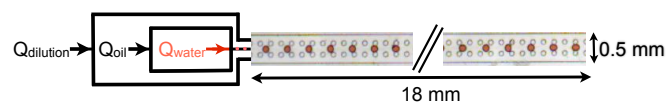


Fig. 1 Design of the microfluidic device. The flow-focusing module is coupled to a dilution module to induce localized jams along the 1D droplet stream, $\phi_0 = 0.22$. Colored water droplets are advected by a Hexadecane phase.

^a PMMH, CNRS UMR 7636, ESPCI ParisTech, Université Paris 6, Université Paris 7, 10, rue Vauquelin, 75231 Paris cedex 05 FRANCE

^b Department of Mechanical and Aerospace Engineering, University of California San Diego, 9500 Gilman Drive, La Jolla CA 92093-0411, USA.

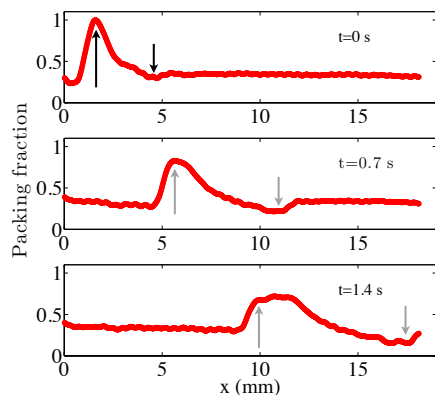


Fig. 2 Time-evolution of the density profiles along the centerline of the channel after a jam induced at $t = 0$. Initial density: $\phi_0 = 0.4$. The arrows follow the position of the maximum/minimum of the initial density perturbations.

resin (NOA 81, Norland optical adhesive)¹⁰. The microchannel is straight, with length $L = 2$ cm, width $W = 500 \mu\text{m}$ and height $h = 70 \mu\text{m}$. Water droplets, colored with a macaroon food-dye, are formed at a conventional flow-focusing junction and injected in the channel (Fig. 1). All the experiments in the paper employ the same droplet diameter, $b = 140 \mu\text{m}$. The continuous phase is a mixture of hexadecane oil (viscosity $\eta = 2\text{mPa}\cdot\text{s}$) and span 80 surfactant (3wt%). The average flow velocity of the continuous phase varies between 5 mm/s and 15 mm/s. The typical Reynolds number is smaller than 10^{-1} , and inertia plays thus a negligible role in the observed dynamics. To focus on longitudinal responses, the droplets are guided by cylindrical posts which impede the transverse destabilization of the crystal (diameter $100 \mu\text{m}$, spacing $100 \mu\text{m}$).

To create a localized longitudinal perturbation (jam) at the entrance of the channel, we use an additional oil inlet to dilute or concentrate dynamically the droplet stream (Fig. 1). Increasing the flow rate in this dilution channel, Q_{dilution} , results in a reduction of the packing fraction. We systematically use the same protocol for the jam formation. First we prepare the system in a stationary state corresponding to a uniform droplet packing-fraction, $\phi(x, t) = \phi_0$. We then suddenly stop the dilution flow for a short period of time. Specifically, Q_{dilution} is set to 0 after a 250 ms linear ramp, kept at the 0 value for 100 ms, and then reset to its initial value after a 250 ms linear ramp. The resulting peak in the local packing fraction, $\phi(x, t)$, and its evolution in time are shown in Fig. 2. Using pictures taken at 60 fps with a 10 bit CMOS camera mounted on a Nikon SMZ1500 stereomicroscope, the density field $\phi(x, t)$ is defined as the instantaneous number of droplets in a rectangular region of size $200 \times 75 \mu\text{m}^2$ centered around the position x and normalized by the number of droplet in the same window

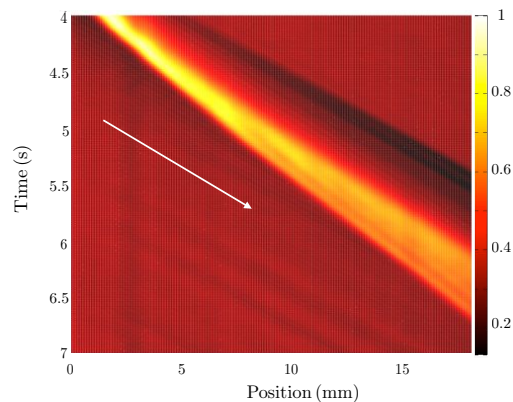


Fig. 3 Spatiotemporal evolution of the density field, $\phi(x, t)$, after a jam induced at $t = 0$ ($\phi_0 = 0.4$ initially). Color map: local density. The white arrow indicates the motion of a droplet far from the jam.

for a close-packed crystal. The position x is defined along the centerline of the channel, with the dilution module connecting the main channel at $x = 0$. The origin of time $t = 0$ is set at the end of the imposed perturbation.

We show in Fig. 2 three snapshots of the density profile illustrating how the local packing fraction, initially in a homogeneous state ($\phi_0 = 0.4$) relaxes after a jam induced at $t = 0$. The full spatiotemporal evolution of the density field within the same experimental conditions is displayed in Fig. 3. Independently of the initial density, all our experiments yield similar phenomenology: the jams are advected along the channel but their shape is not conserved. As seen in Fig. 2, the initial density peak is deformed in an asymmetric manner, with the left front remaining sharp while the right front spreads at a speed comparable to the mean advection velocity. In addition, as the pressure controller used to tune Q_{dilution} systematically induces a minute and brief dilution of the droplet stream prior to the jam formation (see Fig. 2), we also observe an asymmetric spreading of this negative density perturbation.

The dynamic response we observe for both positive and negative density perturbations is not compatible with a linear response to the initial longitudinal excitations, and can thus not be described as the linear superposition of dispersive compression waves (phonons)⁷. The breaking of the left-right symmetry in the spreading dynamics indicates that, instead, a non-linear phenomenon governs the relaxation dynamics of the initial jam. The spatiotemporal evolution of the density field in Fig. 3 shows that the sharp fronts propagate at a constant speed, which we denote V_S , and which depends on the local density ϕ_S at the location of the front. The fronts associated with a positive perturbation propagate slower than the front associated with a negative perturbation. By repeating the same experiment for different ϕ_0 , we can measure the explicit

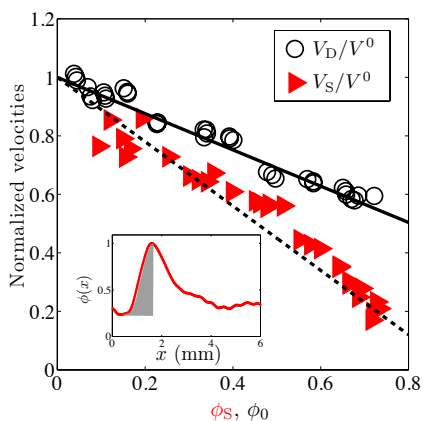


Fig. 4 Red triangles: Positive front velocity, V_S , normalized by the velocity of an isolated drop, vs. the front density ϕ_S . Empty circles: Droplet velocity, in the homogeneous state, V_D , vs. the initial packing fraction, ϕ_0 (same normalization). The error bars are below the symbols size. Solid line: best linear fit. Dashed line: theoretical prediction for the shock velocity. Inset: ϕ_S is defined as the average of $\phi(x)$ over the shaded region.

dependence of the front velocity, V_S , on the local density, ϕ_S , and the results are plotted in Fig. 4 (red triangles). We obtain a clear linear decrease of V_S with ϕ_S , which defines a critical packing fraction, ϕ^* , above which the fronts should propagate upstream, $V_S \equiv V_0(1 - \phi_S/\phi^*)$; note that $V_S(\phi_S = 0) = V_0$ is the velocity of an isolated droplet, which is precisely the velocity of the smallest possible density excitation. A linear fit yield $\phi^* = 0.8$. Experimentally, we could not achieve stable uniform crystal of densities higher than $\phi_0 = 0.7$ over long time scales; above this value, any uncontrolled perturbation leads to transverse destabilization of the 1D streams despite the stabilizing posts. Nonetheless, we measured reductions of the front velocities by a factor of 5 as we increased ϕ_S close to ϕ^* . In addition, the droplet velocity in the homogeneous state, V_D , was observed to decrease linearly with the packing fraction (Fig. 3, open circles). Consequently, the droplets at the rear of the density peak catch up with the jam, where the density is higher and the droplet velocities lower. Simultaneously, the droplets ahead of the jam move faster, resulting in the widening of the density perturbation. This mechanism, akin to Burgers shocks propagation¹¹, is responsible for the formation of stable sharp fronts and asymmetric spreading.

In order to theoretically rationalize our experimental findings, we now introduce a far-field model. We aim at understanding quantitatively how the hydrodynamic coupling between the droplets results in the formation of sharp fronts and the anisotropic spreadings of localized jams. To do so, we derive the local non-linear constitutive equation that relates the density, $\phi(x, t)$, to the droplet current, $j(x, t)$, which

we write without loss of generality as $j(x, t) \equiv \mu u(x, t)\phi(x, t)$, where $u(x, t)$ is the continuous phase velocity, and μ is the droplet mobility. Together with mass conservation, $\partial_t \phi(x, t) + \partial_x j(x, t) = 0$, these two equations determine the nonlinear dynamics of ϕ . For a given channel geometry, μ depends only on the droplet shape. Since the droplets are deformable, μ could implicitly be function of $u(x, t)$, but since the capillary numbers are below 10^{-4} , droplets are not deformed by the continuous flow and μ can be assumed to be a constant. We measure $\mu = 0.7$, which is less than one due to the dissipation in the lubricating film between the droplets and the channel walls, and implies that the droplets disturb the external velocity field, $\mathbf{u}_0(x, t) \equiv u_0 \mathbf{e}_x$, of the continuous phase. The longitudinal component of the flow disturbance, $\delta u(x, t) = u - u_0$, correlates the displacements of the droplets, and is at the origin of the nonlinear dynamics.

To provide an explicit expression for this hydrodynamic coupling, we make two simplifying assumptions. First, having microfluidic applications in mind, we consider mean flows averaged over the height of the channel and thus describe transport by a potential (Hele-Shaw) flow. Second, we assume a dilute suspension of droplets and treat the hydrodynamics in a far-field sense. In that limit, the flow perturbation induced by a droplet at $x = 0$ has the symmetry of a source dipole^{8,9,12}, and induces an instantaneous flow velocity, $u_{\text{dip}}(x)$, at a distance x given by $u_{\text{dip}}(x) = -p/x^2$, if $x \ll W$ where W is the channel width, and $u_{\text{dip}}(x) \sim \exp(-x/W)$, if $x \gg W$ due to hydrodynamic screening by the walls. The dipole strength, p , scales linearly with the area of the droplet in the plane of the flow and with the difference between the droplet speed and that of the surrounding fluid, $p \sim u_0(1 - \mu)b^2$. In the dilute limit, the flow disturbances can be treated as pairwise additives and therefore the flow perturbation induced by all the advected droplets can be written down as a linear superposition of dipolar singularities, $\delta u(x, t) = \int \frac{dx'}{b} \phi(x', t) u_{\text{dip}}(x - x')$. The formula for δu is non-local due to the power-law decay of the hydrodynamic interactions. It also requires regularization at $x = x'$ to model the finite size of the droplets, which we achieve by defining u_{dip} as $u_{\text{dip}}(x, t) \equiv -p/(x^2 + a^2)$ without loss of generality, where $a = b/2$ is the droplet radius.

To derive the local current-density constitutive relation, we consider long-wavelength deformations of the droplet stream. We perform a gradient expansion of the hydrodynamic coupling and write thus the droplet velocity as $\mu \delta u(x, t) = \sum_n a_n \partial_x^n \phi(x, t)$. In the long wavelength limit, the constitutive relation will reduce then to $j = \mu u_0 \phi + a_m \phi(x, t) \partial_x^m \phi(x, t)$, where a_m is the first non zero coefficient of the expansion for the flow perturbation δu . The linear convolution in real space leading to the flow perturbation, $\delta u(x, t)$ is best evaluated in Fourier space where we get $\delta \hat{u}(q, \omega) = b^{-1} \hat{\phi}(q, \omega) \hat{u}_{\text{dip}}(q, \omega)$, where q is the wavenumber, ω the frequency, and $\delta \hat{u}(q, \omega)$ the Fourier transform of $\delta u(x, t)$. Considering longitudinal excita-

tions with wavelengths larger than the cut-off size ($qa \gg 1$) but smaller than the channel width ($qW \ll 1$), we get $\delta\hat{u}(q, \omega) = -(\pi p/ab)\hat{\phi}(q, \omega)e^{-|q|a}$ using the Cauchy theorem. At leading order in qa we have $\delta\hat{u}(q, \omega) = -(\pi p/ab)\hat{\phi}(q, \omega) + O(|qa|)$. In real space and time variables, we obtain therefore that the velocity of the droplets decreases linearly with the packing-fraction as $u(x, t) = u_0 [1 - \pi p/(abu_0)\phi]$. This first prediction is in excellent agreement with the measurements of the droplet velocity in the stationary state (Fig. 4, V_D , open circles). Using this linear relationship, we obtain the local constitutive relation as $j(x, t) = \mu u_0 \phi(x, t) [1 - \frac{1}{2}\phi(x, t)/\phi^*]$, where $\phi^* \equiv abu_0/(2\pi p)$. When combined with mass conservation this leads to the nonlinear equation of motion for the density

$$\partial_t \phi + \mu u_0 \left(1 - \frac{\phi}{\phi^*}\right) \partial_x \phi = 0. \quad (1)$$

Eq. (1) is a Burgers equation for which, as anticipated in the experimental section, the response to a smooth localized density perturbation is a shock wave¹¹. As $\phi^* > 0$, Eq. 1 predicts that an initially symmetric jam evolves to form a sharp front on the upstream side while spreading on the downstream side, in agreement with our experimental observations (Fig. 2). The front velocity is given by $V_S = \mu u_0 (1 - \phi_S/\phi^*)$, where ϕ_S is the average of the packing fractions across the sharp front¹¹. It then follows that $(\partial_{\phi_S} V_S)/(\partial_{\phi_0} V_D) = 1/2$, close to our experimental measurement of 0.55 for this ratio (Fig. 4). The agreement between our experimental observations and our theoretical predictions demonstrates thus that the nonlinear response of a 1D droplet stream can be described by a Burgers dynamics arising from long-range hydrodynamic interactions.

Although our experiments did not allow to probe higher order terms in the gradient expansion, we can theoretically compute the dispersion relation of the compression waves at all orders in qa . Searching for Fourier modes as $\phi(x, t) = \phi_0 + \varepsilon \exp(i\omega t - iqx)$, we obtain to first order in ε perturbations propagating in a dispersive manner along the 1D stream^{7,8}, with a dispersion relation $\omega = u_0 q \left[1 - \frac{\phi_0}{2\phi^*} (1 + e^{-|q|a})\right]$. Note however that 1D hydrodynamic crystals having more than one spatial period and long wavelength modulations are not stationary solutions of Eq. (1), and any long wavelength density modulation would ultimately form localized shocks.

Our results have implications beyond our immediate experimental investigation. The Burgers phenomenology is not specific to particles advected by potential flows. The leading order term in the gradient expansion of $\delta u(x, t)$ always scales as $\phi(x, t)$ provided that the elementary flow perturbation is an even function of x (a_0 represents the spatial average of the flow perturbation induced by an isolated particle). Our predictions do therefore not depend on the specifics of the shape of the channel boundaries. More importantly, particles driven by external forces (gravitational, electric, magnetic,...) should

follow a similar large scale dynamic, both in confined geometries and in unbounded fluids. Notably, the sign of the induced dipole depends on the details of the driving. Specifically, p is positive (resp. negative) for particles moving slower (resp. faster) than the surrounding fluid. A stream of particles driven by an external force (or self-propelling) in a quiescent fluid could be flowed at arbitrarily high current value, as in this case the $j(\phi)$ function has no upper bound, $j(\phi) = \mu u_0 \phi(x, t) [1 + \frac{1}{2}\phi(x, t)/\phi^*]$, and would lead to fast shocks propagating at a finite velocity, $V_S = \mu u_0 (1 + \phi_S/\phi^*)$, for all densities as observed in 2D particle streams¹³. In contrast, for advected particles, there exists a maximum current, $j(\phi^*)$, to the quadratic constitutive relation⁹, and the shock velocity V_S vanishes when $\phi \rightarrow \phi^*$, leading to long-lived density perturbations with lifetime $\sim (1 - \phi_0/\phi^*)^{-1}$. Digital microfluidic setups in which particles are driven by external fields, although they might require involved fabrication steps, would thus be more robust to longitudinal density perturbations.

This work was funded in part by the Paris Emergence 2009 program, the C’Nano Ile de France DypMoA research grant, and the National Science Foundation (grant CBET-0746285).

References

- 1 C. Simonet and A. Groisman, *Anal. Chem.*, **78**, 5653 (2006) and references therein.
- 2 L.-H. Hung, S.-Y. Teh, R. Lin and A. P. Lee, *Lab Chip*, **8**, 198 (2008).
- 3 D. Dendukuri, and P. S. Doyle, *Adv. Mater.*, **21**, 4071(2009)
- 4 P. Abbyad, R. Dangla, A. Alexandrou and C. N. Baroud *Lab Chip*, **11**, 813 (2011)
- 5 C. Baroud, F. Gallaire, and R. Dangla, *Lab Chip*, **10**, 2032 (2010)
- 6 S. E Chung, W. Park, S. Shin, S. A. Lee, and S. Kwon *Nat. Mater.*, **7**, 581 (2007).
- 7 T. Beatus, T. Tlusty, and R. Bar-Ziv, *Nature Phys.*, **2**, 743 (2006)
- 8 T. Beatus, R. Bar-Ziv, and T. Tlusty, *Phys. Rev. Lett.*, **99**, 124502, (2007)
- 9 N. Champagne, R. Vasseur, A. Montourcy, and D. Bartolo, *Phys. Rev. Lett.*, **105**, 044502, 2010
- 10 D. Bartolo, G. Degré, P. Nghe, and V. Studer *Lab Chip*, **8**, 274 (2008)
- 11 G. B. Witham, *Linear and Nonlinear Waves*, Wiley-Interscience, (1974)
- 12 N. Liron and S. Mochon *J. Eng. Math.*, **10**, 287, (1976)
- 13 T. Beatus, T. Tlusty, and R. Bar-Ziv *Phys. Rev. Lett.*, **103**, 114502, (2009). The mechanisms responsible for the reversal of the shocks polarity in 2D streams will be discussed in a forthcoming paper.